PHYSICAL REVIEW D **72,** 051109(R) (2005)

Measurement of the branching fractions for $B^- \to D^{(*)+}\pi^-\ell^-\bar{\nu}_\ell$ and $\bar{B}^0 \to D^{(*)0}\pi^+\ell^-\bar{\nu}_\ell$

D. Liventsev,[8] T. Matsumoto,[40] K. Abe,[5] K. Abe,[36] H. Aihara,[38] Y. Asano,[42] T. Aushev,[8] A. M. Bakich,[33] V. Balagura,[8] M. Barbero,[4] I. Bedny,[1] U. Bitenc,[9] I. Bizjak,[9] S. Blyth,[18] A. Bondar,[1] M. Bračko,[5,14,9] T. E. Browder,[4] Y. Chao,[20] A. Chen,[18] W. T. Chen,[18] B. G. Cheon,[2] R. Chistov,[8] Y. Choi,[32] A. Chuvikov,[29] S. Cole,[33] J. Dalseno,[15] M. Dash,[43] L. Y. Dong,[6] S. Eidelman,[1] Y. Enari,[16] S. Fratina,[9] N. Gabyshev,[1] T. Gershon,[5] A. Go,[18] G. Gokhroo,[34] J. Haba,[5] T. Hara,[26] K. Hayasaka,[16] H. Hayashii,[17] M. Hazumi,[5] L. Hinz,[12] T. Hokuue,[16] Y. Hoshi,[36] S. Hou,[18] W.-S. Hou,[20] T. Iijima,[16] K. Ikado,[16] A. Imoto,[17] A. Ishikawa,[5] R. Itoh,[5] M. Iwasaki,[38] J. H. Kang,[44] J. S. Kang,[11] S. U. Kataoka,[17] T. Kawasaki,[23] H. R. Khan,[39] H. Kichimi,[5] S. M. Kim,[32] K. Kinoshita,[3] P. Križan,[13,9] P. Krokovny,[1] C. C. Kuo,[18] A. Kuzmin,[1] Y.-J. Kwon,[44] T. Lesiak,[21] S.-W. Lin,[20] F. Mandl,[7] A. Matyja,[21] W. Mitaroff,[7] H. Miyake,[26] H. Miyata,[23] Y. Miyazaki,[16] R. Mizuk,[8] E. Nakano,[25] M. Nakao,[5] Z. Natkaniec,[21] S. Nishida,[5] O. Nitoh,[41] T. Nozaki,[5] S. Ogawa,[35] T. Ohshima,[16] T. Okabe,[16] S. Okuno,[10] S. L. Olsen,[4] Y. Onuki,[23] W. Ostrowicz,[21] H. Ozaki,[5] P. Pakhlov,[8] H. Palka,[21] C. W. Park,[32] N. Parslow,[33] R. Pestotnik,[9] L. E. Piilonen,[43] F. J. Ronga,[5] M. Rozanska,[21] Y. Sakai,[5] N. Sato,[16] N. Satoyama,[31] K. Sayeed,[3] T. Schietinger,[12] O. Schneider,[12] C. Schwanda,[7] H. Shibuya,[35] B. Shwartz,[1] A. Somov,[3] N. Soni,[27] S. Stanič,[24] M. Starič,[9] T. Sumiyoshi,[40] S. Y. Suzuki,[5] K. Tamai,[5] N. Tamura,[23] M. Tanaka,[5] Y. Teramoto,[25] X. C. Tian,[28] T. Tsukamoto,[5] S. Uehara,[5] T. Uglov,[8] K. Ueno,[20] Y. Unno,[5] S. Uno,[5] P. Urquijo,[15] G. Varner,[4] K. E. Varvell,[33] S. Villa,[12] C. H. Wang,[19] M.-Z. Wang,[20] Y. Watanabe,[39] E. Won,[11] Q. L. Xie,[6] A. Yamaguchi,[37] Y. Yamashita,[22] M. Yamauchi,[5] J. Ying,[28] L. M. Zhang,[30] Z. P. Zhang,[30] and V. Zhilich[1]

(Belle Collaboration)

[1]*Budker Institute of Nuclear Physics, Novosibirsk*
[2]*Chonnam National University, Kwangju*
[3]*University of Cincinnati, Cincinnati, Ohio 45221, USA*
[4]*University of Hawaii, Honolulu, Hawaii 96822, USA*
[5]*High Energy Accelerator Research Organization (KEK), Tsukuba*
[6]*Institute of High Energy Physics, Chinese Academy of Sciences, Beijing*
[7]*Institute of High Energy Physics, Vienna*
[8]*Institute for Theoretical and Experimental Physics, Moscow*
[9]*J. Stefan Institute, Ljubljana*
[10]*Kanagawa University, Yokohama*
[11]*Korea University, Seoul*
[12]*Swiss Federal Institute of Technology of Lausanne, EPFL, Lausanne*
[13]*University of Ljubljana, Ljubljana*
[14]*University of Maribor, Maribor*
[15]*University of Melbourne, Victoria*
[16]*Nagoya University, Nagoya*
[17]*Nara Women's University, Nara*
[18]*National Central University, Chung-li*
[19]*National United University, Miao Li*
[20]*Department of Physics, National Taiwan University, Taipei*
[21]*H. Niewodniczanski Institute of Nuclear Physics, Krakow*
[22]*Nippon Dental University, Niigata*
[23]*Niigata University, Niigata*
[24]*Nova Gorica Polytechnic, Nova Gorica*
[25]*Osaka City University, Osaka*
[26]*Osaka University, Osaka*
[27]*Panjab University, Chandigarh*
[28]*Peking University, Beijing*
[29]*Princeton University, Princeton, New Jersey 08544, USA*
[30]*University of Science and Technology of China, Hefei*
[31]*Shinshu University, Nagano*
[32]*Sungkyunkwan University, Suwon*
[33]*University of Sydney, Sydney NSW*
[34]*Tata Institute of Fundamental Research, Bombay*
[35]*Toho University, Funabashi*
[36]*Tohoku Gakuin University, Tagajo*

[37]*Tohoku University, Sendai*
[38]*Department of Physics, University of Tokyo, Tokyo*
[39]*Tokyo Institute of Technology, Tokyo*
[40]*Tokyo Metropolitan University, Tokyo*
[41]*Tokyo University of Agriculture and Technology, Tokyo*
[42]*University of Tsukuba, Tsukuba*
[43]*Virginia Polytechnic Institute and State University, Blacksburg, Virginia 24061, USA*
[44]*Yonsei University, Seoul*

(Received 16 August 2005; published 30 September 2005)

We report on a measurement of the branching fractions for $B^- \to D^{(*)+}\pi^-\ell^-\bar{\nu}_\ell$ and $\bar{B}^0 \to D^{(*)0}\pi^+\ell^-\bar{\nu}_\ell$ with 275×10^6 $B\bar{B}$ events collected at the $\Upsilon(4S)$ resonance with the Belle detector at KEKB. Events are tagged by fully reconstructing one of the B mesons in hadronic modes. We obtain $\mathcal{B}(B^- \to D^+\pi^-\ell^-\bar{\nu}_\ell) = (0.54 \pm 0.07(\text{stat}) \pm 0.07(\text{syst}) \pm 0.06(\text{BR})) \times 10^{-2}$, $\mathcal{B}(B^- \to D^{*+}\pi^-\ell^-\bar{\nu}_\ell) = (0.67 \pm 0.11(\text{stat}) \pm 0.09(\text{syst}) \pm 0.03(\text{BR})) \times 10^{-2}$, $\mathcal{B}(\bar{B}^0 \to D^0\pi^+\ell^-\bar{\nu}_\ell) = (0.33 \pm 0.06(\text{stat}) \pm 0.06(\text{syst}) \pm 0.03(\text{BR})) \times 10^{-2}$, $\mathcal{B}(\bar{B}^0 \to D^{*0}\pi^+\ell^-\bar{\nu}_\ell) = (0.65 \pm 0.12(\text{stat}) \pm 0.08(\text{syst}) \pm 0.05(\text{BR})) \times 10^{-2}$, where the third error comes from the error on $\bar{B} \to D^{(*)}\ell^-\bar{\nu}_\ell$ decays. Contributions from $\bar{B}^0 \to D^{*+}\ell^-\bar{\nu}_\ell$ decays are excluded in the measurement of $\bar{B}^0 \to D^0\pi^+\ell^-\bar{\nu}_\ell$.

DOI: 10.1103/PhysRevD.72.051109 PACS numbers: 13.20.He

Semileptonic decays play a prominent role in the study of B meson properties. The total semileptonic branching fraction has been precisely determined to be $(10.73 \pm 0.28) \times 10^{-2}$ [1]. While $\bar{B} \to D\ell^-\bar{\nu}_\ell$ and $D^*\ell^-\bar{\nu}_\ell$ account for 70% of this total, other contributions are not yet well understood. The most promising candidates include resonant and nonresonant $D^{(*)}\pi$ in the final state. Both ALEPH [2] and DELPHI [3] have studied $\bar{B} \to D^{(*)}\pi\ell^-\bar{\nu}_\ell$ decays (where both $\pi^\pm$ and π^0 modes are included). Assuming that semileptonic B decays other than $\bar{B} \to D\ell^-\bar{\nu}_\ell$ and $\bar{B} \to D^*\ell^-\bar{\nu}_\ell$ are of the form $\bar{B} \to D^{(*)}\pi\ell^-\bar{\nu}_\ell$, they find:

$$\begin{aligned}\mathcal{B}_{D^{(*)}\pi\ell^-\bar{\nu}_\ell} &\equiv \mathcal{B}(\bar{B} \to D\pi\ell^-\bar{\nu}_\ell) + \mathcal{B}(\bar{B} \to D^*\pi\ell^-\bar{\nu}_\ell) \\ &= (2.16 \pm 0.30 \pm 0.30) \times 10^{-2}(\text{ALEPH}), \\ &= (3.40 \pm 0.52 \pm 0.32) \times 10^{-2}(\text{DELPHI}).\end{aligned}$$

The former result suggests that there is a significant unknown contribution to the semileptonic branching fraction, while the latter shows no such deficit. More precise measurements are therefore desired to resolve this discrepancy and clarify the difference between the rate for the inclusive semileptonic decay and the sum of the rates for the exclusive modes. Improvement in the knowledge of the $\bar{B} \to D^{(*)}\pi\ell^-\bar{\nu}_\ell$ branching fractions will also help to reduce systematic uncertainties in measurements of Cabibbo-Kobayashi-Maskawa elements such as $|V_{cb}|$ and $|V_{ub}|$ [4].

In this paper, we present measurements of the branching fractions for $\bar{B} \to D^{(*)}\pi\ell^-\bar{\nu}_\ell$ decays. Inclusion of charge conjugate decays is implied throughout the paper. The analysis is based on data collected with the Belle detector [5] at the KEKB e^+e^- asymmetric collider [6]. We use a 253 fb^{-1} data sample at the $\Upsilon(4S)$ resonance ($\sqrt{s} \simeq 10.58$ GeV), corresponding to a sample of 275×10^6 $B\bar{B}$ pairs. The selection of hadronic events is described elsewhere [7]. An additional 28 fb^{-1} data sample taken at a center-of-mass energy 60 MeV below the $\Upsilon(4S)$ resonance is also used to study continuum $e^+e^- \to q\bar{q}(q = u, d, s, c)$ events.

The Belle detector is a large-solid-angle spectrometer with a 1.5 T magnetic field provided by a superconducting solenoid coil. Charged particles are measured using hits in a silicon vertex detector (SVD) and a 50-layer central drift chamber (CDC). Photons are detected in an electromagnetic calorimeter (ECL) comprised of CsI(Tl) crystals. Kaon identification is performed by combining the responses from an array of aerogel threshold Čerenkov counters (ACC), a barrel-like arrangement of time-of-flight scintillation counters (TOF), and dE/dx measurements in the CDC. A K/π likelihood ratio $P_{K/\pi}$, ranging from 0 (likely to be a pion) to 1 (likely to be a kaon), is formed. With the requirement $P_{K/\pi} > 0.6$, the kaon efficiency is approximately 88% and the average pion misidentification rate is about 8%. Electron identification is based on a combination of dE/dx in CDC, the response of ACC, shower shape in ECL, and the ratio of energy deposit in ECL to the momentum measured by the tracking system. Muon identification is performed using resistive counters interleaved in the iron yoke, located outside the coil. The lepton identification efficiencies are about 90% for both electrons and muons in the momentum region above 1.2 GeV/c, where leptons from the prompt B decays dominate. The hadron misidentification rate is less than 0.5% for electrons and 2% for muons in the same momentum region.

We use a GEANT-based Monte Carlo (MC) simulation to model the response of the detector and determine its acceptance [8]. $\bar{B} \to D^{(*)}\ell^-\bar{\nu}_\ell$ and $D^{(*)}\pi\ell^-\bar{\nu}_\ell$ events are modeled using the EvtGen program [9]. We use an HQET-based model [10] for $\bar{B} \to D^{(*)}\ell^-\bar{\nu}_\ell$ and the Goity-Roberts model [11] for $\bar{B} \to D^{(*)}\pi\ell^-\bar{\nu}_\ell$. $\bar{B} \to D^{**}(\to D^{(*)}\pi)\ell^-\bar{\nu}_\ell$ is also simulated using the ISGW model [12] to evaluate the model dependence.

To suppress the high combinatorial background expected in the reconstruction of final states including a neutrino, we fully reconstruct one of the B mesons, referred to hereafter as the *tag*. This allows us to separate particles created in the tag decay from those used in reconstructing the semileptonic decay, which we call *signal*. It also provides a measurement of the momentum of the signal B meson, thus greatly improving the resolution on the missing momentum.

The tag is fully reconstructed in the following modes: $B^+ \to \bar{D}^{(*)0}\pi^+$, $\bar{D}^{(*)0}\rho^+$, $\bar{D}^{(*)0}a_1^+$, $\bar{D}^{(*)0}D_s^{(*)+}$, and $B^0 \to D^{(*)-}\pi^+$, $D^{(*)-}\rho^+$, $D^{(*)-}a_1^+$, $D^{(*)-}D_s^{(*)+}$. $\bar{D}^0$ candidates are reconstructed in seven modes: $\bar{D}^0 \to K^+\pi^-$, $K^+\pi^-\pi^0$, $K^+\pi^+\pi^+\pi^-$, $K_S^0\pi^0$, $K_S^0\pi^+\pi^-$, $K_S^0\pi^+\pi^-\pi^0$, K^+K^-. D^- candidates are reconstructed in six modes: $D^- \to K^+\pi^-\pi^-$, $K^+\pi^+\pi^-\pi^0$, $K_S^0\pi^-$, $K_S^0\pi^-\pi^0$, $K_S^0\pi^+\pi^-\pi^-$, $K^+K^-\pi^-$. D_s^+ candidates are reconstructed in $D_s^+ \to K_S^0K^+$, $K^+K^-\pi^+$. The D candidates are required to have an invariant mass m_D within $\pm 4-5\sigma$ of the nominal D mass value depending on the mode. D^* mesons are reconstructed in the $D^{*+} \to D^0\pi^+/D^+\pi^0$, $D^{*0} \to D^0\pi^0/D^0\gamma$ and $D_s^{*+} \to D_s^+\gamma$ decays. D^* candidates from modes that include a pion are required to have a mass difference $\Delta m = m_{D\pi} - m_D$ within ± 5 MeV$/c^2$ of its nominal value. For the decays with a photon, we require that the mass difference $\Delta m = m_{D\gamma} - m_D$ be within ± 20 MeV$/c^2$ of the nominal value.

The selection of the tag candidates is based on $M_{\rm bc} = \sqrt{E_{\rm beam}^2 - p_B^2}$ and $\Delta E = E_B - E_{\rm beam}$, where $E_{\rm beam} \equiv \sqrt{s}/2 \simeq 5.29$ GeV, and p_B and E_B are the momentum and energy of the reconstructed B in the $\Upsilon(4S)$ rest frame, respectively. The background from jetlike continuum events is suppressed on the basis of event topology: we require the normalized second Fox-Wolfram moment [13] to be smaller than 0.5, and $|\cos\theta_{\rm th}| < 0.8$, where $\theta_{\rm th}$ is the angle between the thrust axis of the B candidate and that of the remaining tracks in an event. The latter requirement is not applied to $B^+ \to \bar{D}^0\pi^+, \bar{D}^{*0}(\to \bar{D}^0\pi^0)\pi^+$ and $B^0 \to D^{*-}(\to \bar{D}^0\pi^-)\pi^+$ decays, where this background is smaller.

The signal region for tag candidates is defined as $M_{\rm bc} > 5.27$ GeV$/c^2$ and -80 MeV $< \Delta E < 60$ MeV. If an event has multiple B candidates, we choose for each of B^+ and B^0 the candidate with the smallest χ^2 based on the deviations from the nominal values of ΔE, m_D, and Δm if applicable.

Figure 1 shows the distribution in $M_{\rm bc}$ of B^+ and B^0 candidates in the ΔE signal region. The number of tagged events is obtained by fitting the distribution with empirical functions: a Crystal Ball function for signal [14] and an ARGUS function for background [15]. The fits yield $(4.26 \pm 0.17) \times 10^5$ B^+, with a purity of 55%, and $(2.72 \pm 0.11) \times 10^5$ B^0, with a purity of 50%. These yields include cross-feeds between B^+ and B^0; these peak in $M_{\rm bc}$ and are not well separated by fitting. From the MC simulation, we estimate the fraction of B^0 (B^+) events in the reconstruction of B^+ (B^0) to be 0.095 (0.090). The corrected yields of tags are: $N_{\rm tag} = (3.88 \pm 0.20) \times 10^5$ for B^+ and $N_{\rm tag} = (2.46 \pm 0.12) \times 10^5$ for B^0.

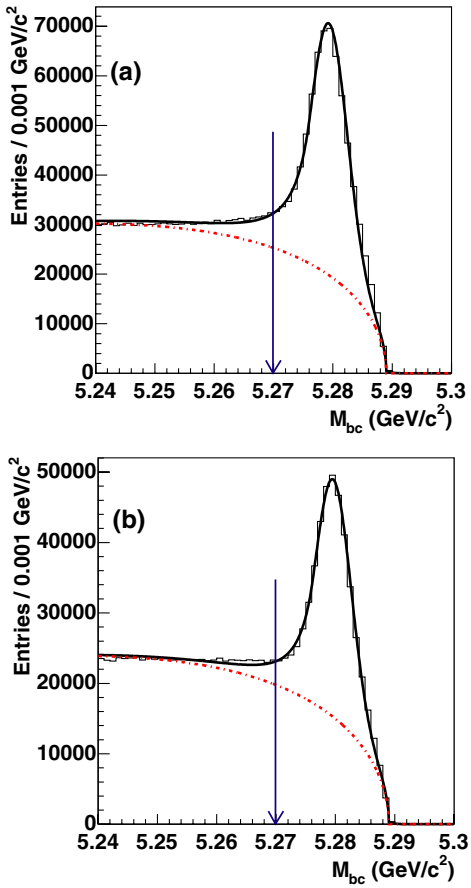

FIG. 1 (color online). $M_{\rm bc}$ distributions for fully reconstructed hadronic (a) B^+ and (b) B^0 decays. The solid curve is the sum of the fitted signal and background components, the dashed curve is the fitted background component. The signal region is indicated by solid arrows.

On the signal side, we reconstruct the following modes: $B^- \to D^{(*)0}\ell^-\bar{\nu}_\ell$, $D^{(*)+}\pi^-\ell^-\bar{\nu}_\ell$, and $\bar{B}^0 \to D^{(*)+}\ell^-\bar{\nu}_\ell$, $D^{(*)0}\pi^+\ell^-\bar{\nu}_\ell$. $\bar{B} \to D^{(*)}\ell^-\bar{\nu}_\ell$ decays are reconstructed as control samples to determine experimental resolutions, evaluate systematic errors, and normalize the results. All modes are reconstructed with all remaining particles after the full reconstruction of the tag. Flavor combinations of the two B mesons are restricted to B^+B^-, $B^0\bar{B}^0$, B^0B^0 and $\bar{B}^0\bar{B}^0$. We do not require opposite flavor for neutral B mesons because of the effect of mixing.

The selection of $D^{(*)}$ mesons is performed in the same manner as for the tag. We require that lepton candidates be identified as electrons or muons and have momentum

greater than 0.6 GeV/c in the laboratory frame. The electron and muon with largest momentum are selected as lepton candidates in each event. The pion candidates are selected with a loose criterion, $P_{K/\pi} < 0.9$. We select the B meson candidate formed with the best $D^{(*)}$ candidate (smallest χ^2 of the deviations from the nominal values of m_D, and Δm_D if applicable), and require that no charged track be left unused. Additionally, in the case of $\bar{B}^0 \to D^0\pi^+\ell^-\bar{\nu}_\ell$ and $D^{*0}(\to D^0\pi^0, D^0\gamma)\pi^+\ell^-\bar{\nu}_\ell$ reconstructions, we require $M(D^0\pi^+) > 2.1$ GeV/c^2 to veto events from $\bar{B}^0 \to D^{*+}\ell^-\bar{\nu}_\ell$.

The semileptonic decay is identified by the missing mass squared, $M^2_{\rm miss} = (E_{\rm beam} - E_{D^{(*)}(\pi)} - E_{\ell^-})^2 - (\mathbf{P}_{B_{\rm tag}} + \mathbf{P}_{D^{(*)}(\pi)} + \mathbf{P}_{\ell^-})^2$, where $E_{\rm beam}$ is the above-mentioned beam energy, $E_{D^{(*)}(\pi)}$ and E_{ℓ^-} are the $D^{(*)}(\pi)$ and lepton energies, and $\mathbf{P}_{D^{(*)}(\pi)}$ and $\mathbf{P}_{\ell^-}$ are the corresponding 3-momenta. $\mathbf{P}_{B_{\rm tag}}$ is the 3-momentum of the tag. All these variables are calculated in the $\Upsilon(4S)$ rest frame. For the signal, $M^2_{\rm miss}$ peaks around zero. The resolution on $M^2_{\rm miss}$ ranges from 0.03 to 0.07 GeV$^2/c^4$, depending on the mode. In contrast, previous analyses (e.g. by the ARGUS collaboration [16]), in which the $\mathbf{P}_{B_{\rm tag}}$ term was neglected, led to a resolution of $\sim$0.5 GeV$^2/c^4$ on $M^2_{\rm miss}$. This very good $M^2_{\rm miss}$ resolution allows reduction of the combinatorial background and to separate semileptonic decays that differ by only one pion or γ in the final state. The distributions in $M^2_{\rm miss}$ for $\bar{B} \to D^{(*)}\ell^-\bar{\nu}_\ell$ and $D^{(*)}\pi\ell^-\bar{\nu}_\ell$ are shown in Figs. 2 and 3. The signal events are clearly evident.

We have investigated the backgrounds from $B\bar{B}$ and continuum events using MC simulation and off-resonance data. There are four main sources of background:

(1) Semileptonic B decays where a pion or a photon is missed (e.g. $\bar{B} \to D^*(\pi)\ell^-\bar{\nu}_\ell$ reconstructed as $\bar{B} \to D(\pi)\ell^-\bar{\nu}_\ell$ if the soft π^0 or γ from D^* is missed). These distribute at high values of $M^2_{\rm miss}$ and can therefore be distinguished from signal.

(2) Semileptonic B decays where a random photon candidate is used in D^{*0} reconstruction (i.e. $\bar{B} \to D^0(\pi)\ell^-\bar{\nu}_\ell$ is reconstructed as $\bar{B} \to D^{*0}(\pi)\ell^-\bar{\nu}_\ell$). These events have a lower value of $M^2_{\rm miss}$.

(3) Hadronic decays $\bar{B} \to D^{(*)}nh$ where one of the hadrons is misidentified as a lepton. These events peak near $M^2_{\rm miss} = 0$ and therefore need special care as described below.

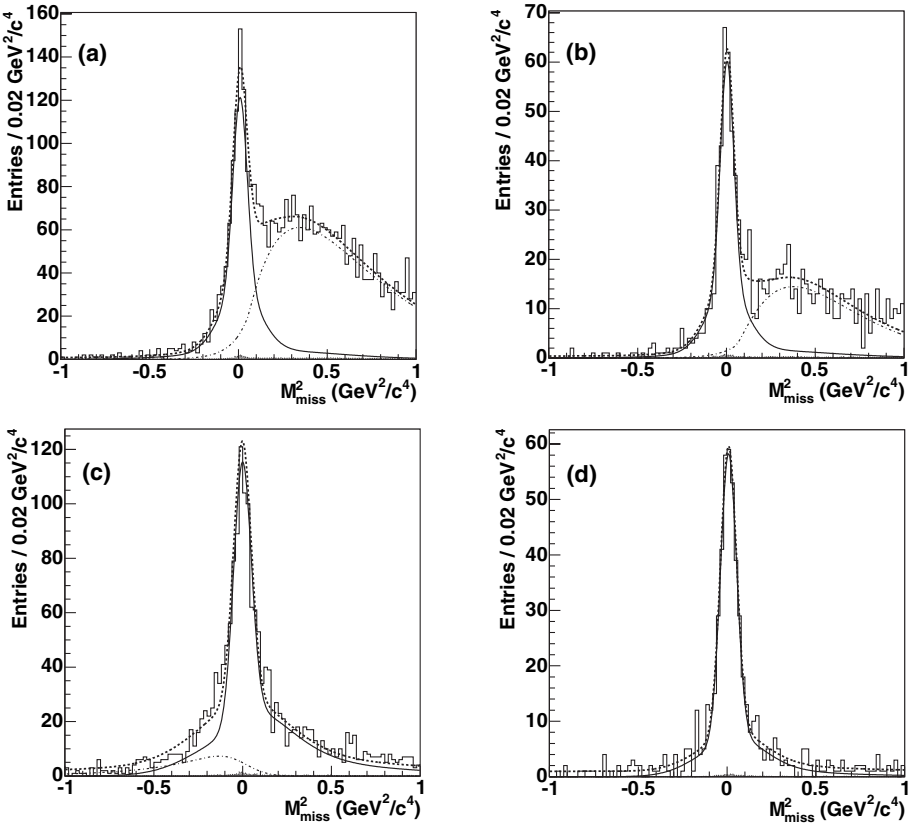

FIG. 2. $M^2_{\rm miss}$ distributions for (a) $B^- \to D^0\ell^-\bar{\nu}_\ell$, (b) $\bar{B}^0 \to D^+\ell^-\bar{\nu}_\ell$, (c) $B^- \to D^{*0}\ell^-\bar{\nu}_\ell$ and (d) $\bar{B}^0 \to D^{*+}\ell^-\bar{\nu}_\ell$. Data are plotted as a histogram, and the fit result is overlaid as a dotted line. Signal (solid curve), other semileptonic decays (dash-dotted) and misidentified hadronic events (shaded histogram) are also shown.

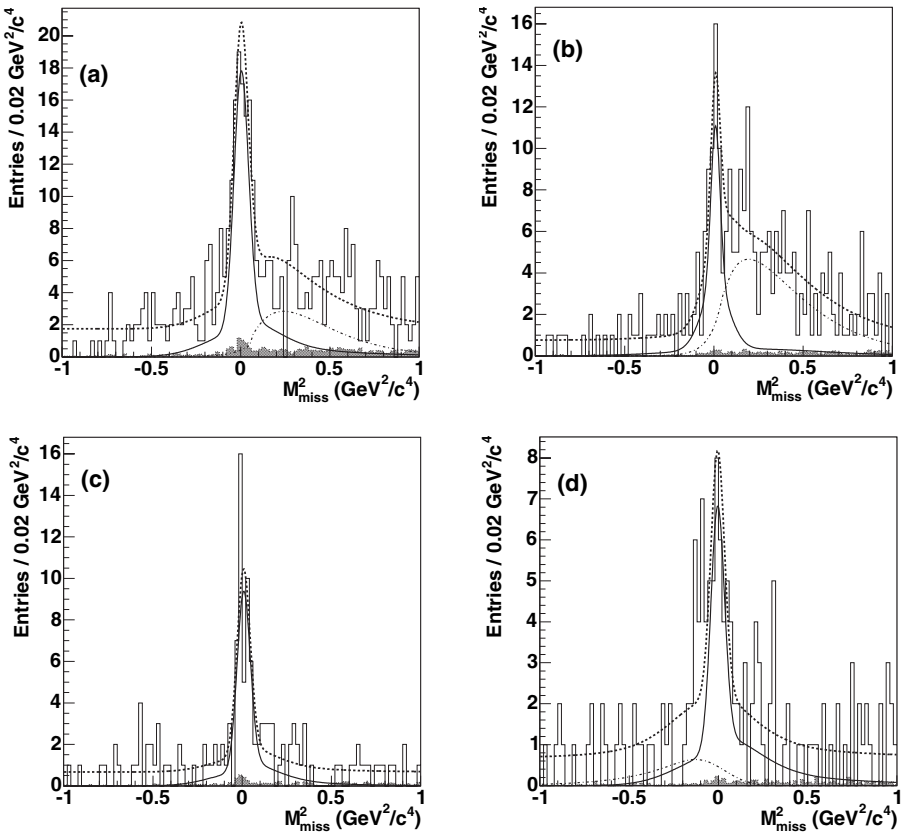

FIG. 3. $M^2_{\rm miss}$ distributions for (a) $B^- \to D^+\pi^-\ell^-\bar{\nu}_\ell$, (b) $\bar{B}^0 \to D^0\pi^+\ell^-\bar{\nu}_\ell$, (c) $B^- \to D^{*+}\pi^-\ell^-\bar{\nu}_\ell$ and (d) $\bar{B}^0 \to D^{*0}\pi^+\ell^-\bar{\nu}_\ell$. Distributions are shown as described in Fig. 2.

(4) Random combinations. As the tag is fully reconstructed, this background is expected to be small. The distribution in $M^2_{\rm miss}$ is studied using events in the ΔE side-band ($0.1\ {\rm GeV} < \Delta E < 0.3\ {\rm GeV}$) and off-resonance data. It is found to be consistent with a flat distribution in $M^2_{\rm miss}$.

The signal yields are obtained by a binned maximum likelihood fit to the $M^2_{\rm miss}$ distributions in the interval $[-1.0, 1.0]\ {\rm GeV}^2/c^4$. The total fit function is: $F(x \equiv M^2_{\rm miss}) = (N_{\rm sig} + N_{\rm bkg3})S(x) + N_{\rm bkg1}B_1(x) + N_{\rm bkg2}B_2(x) + N_{\rm bkg4}B_4(x)$, where $N_{\rm sig}$ is the number of signal events and the $N_{\rm bkg(n)}$ are the number of background events corresponding to categories 1–4 listed above. The signal shape $S(x)$ is a sum of two Gaussians and a single-sided exponential convolved with a Gaussian; the smeared exponential is necessary to describe the upper tail, which is due to energy loss, mainly by radiation from the electron. $B_i(x)$ are normalized background shapes. For $B_1(x)$, we use a threshold function ($\propto x^\alpha \exp(-\beta x)$), plus an exponential function to describe the lower tail component at $M^2_{\rm miss} \simeq 0\ {\rm GeV}^2/c^4$. $B_2(x)$ is a smeared exponential function. $B_4(x)$ is constant in the fitted interval.

$N_{\rm sig}$, $N_{\rm bkg1}$ and $N_{\rm bkg4}$ are floated in the fit, while $N_{\rm bkg2}$ and $N_{\rm bkg3}$ are determined from data and fixed. (According to our background categorization, $N_{\rm bkg1}$ ($N_{\rm bkg2}$) is nonzero only for $\bar{B} \to D(\pi)\ell^-\bar{\nu}_\ell$ ($\bar{B} \to D^{*0}(\pi)\ell^-\bar{\nu}_\ell$) decays.) The shape parameters of $B_1(x)$ and $B_2(x)$ are fixed using MC simulations. The mean and width of $S(x)$ are floated in the fit to $\bar{B} \to D^{(*)}\ell^-\bar{\nu}_\ell$, and the observed discrepancies with MC simulations are used to fix the mean and width of $S(x)$ for $\bar{B} \to D^{(*)}\pi\ell^-\bar{\nu}_\ell$. Other shape parameters of $S(x)$ are determined from MC simulations.

To determine $N_{\rm bkg2}$ we multiply the measured number of $\bar{B} \to D^0(\pi)\ell^-\bar{\nu}_\ell$ events by the probability of such events faking $\bar{B} \to D^{*0}(\pi)\ell^-\bar{\nu}_\ell$, as determined in MC simulations. To determine the contribution from misidentified hadronic decays ($N_{\rm bkg3}$), we use a sample of events which are reconstructed as signal but where the lepton candidates do not pass the identification requirement. We weight these events by lepton misidentification rates binned in laboratory momentum, as determined from a control sample of $D^{*+} \to D^0(\to K^-\pi^+)\pi^+$ events. (In the case of $B^- \to D^{(*)+}\pi^-\ell^-\bar{\nu}_\ell$, we also consider the possibility that the prompt pion is misidentified as a lepton.) $N_{\rm bkg3}$ is then

determined by a fit to the $M^2_{\rm miss}$ distributions of this special sample.

The results for $\bar{B} \to D^{(*)}\ell^-\bar{\nu}_\ell$ and $\bar{B} \to D^{(*)}\pi\ell^-\bar{\nu}_\ell$ are shown in Fig. 2 and 3 and listed in Table I and II. The statistical significance of the signal yield is defined as $\Sigma = \sqrt{2\ln(-L_0/L_{\rm max})}$, where $L_{\rm max}$ and L_0 denote the maximum likelihood value and likelihood value obtained assuming zero signal events, respectively. Signals are observed in all $\bar{B} \to D^{(*)}\pi\ell^-\bar{\nu}_\ell$ modes with a statistical significance of more than 7.

The raw branching fractions are calculated as $\mathcal{B} = N_{\rm sig}/(2\epsilon N_{\rm tag})$, where $N_{\rm sig}$ is the measured number of $\bar{B} \to D^{(*)}(\pi)\ell^-\bar{\nu}_\ell$ events and $N_{\rm tag}$ is the number of selected tags. The efficiency ϵ is defined as $\epsilon \equiv \epsilon^{\rm signal} \times \epsilon^{\rm signal}_{\rm frec}/\epsilon^{\rm generic}_{\rm frec}$, where $\epsilon^{\rm generic}_{\rm frec}$ is fully reconstructed tagging efficiency and $\epsilon^{\rm signal}_{\rm frec}$ is its efficiency in the case of one B decays into the signal mode. The factor $\epsilon^{\rm signal}_{\rm frec}/\epsilon^{\rm generic}_{\rm frec}$ accounts for the difference of B tagging efficiency between the signal decay modes and generic B decays and is estimated to be around 1.05 depending on the mode. The obtained raw branching fractions in normalization modes, $\bar{B} \to D^{(*)}\ell^-\bar{\nu}_\ell$ are shown in Table I. These agree with the world average values quoted in Ref. [1].

To calculate the branching fractions for $\bar{B} \to D^{(*)}\pi\ell^-\bar{\nu}_\ell$, we first find the ratio R of the raw branching fractions for each of these decays to that of the $\bar{B} \to D^{(*)}\ell^-\bar{\nu}_\ell$ decay mode with the same $D^{(*)}$ charge, then multiply R by the world average values of $\mathcal{B}(\bar{B} \to D^{(*)}\ell^-\bar{\nu}_\ell)$ [1]. The results are shown in Table III.

Systematic errors in the measurement of the branching fractions for $\bar{B} \to D^{(*)}\pi\ell^-\bar{\nu}_\ell$ are associated with the uncertainties in the signal yields, tag yields, and reconstruction efficiencies. Most of the systematic errors related to the reconstruction of the $D^{(*)}$ and the lepton, as well as the branching fraction of the $D^{(*)}$ decays, cancel out in the ratio R.

Systematic errors in the signal yields are estimated from uncertainties in the signal shape, background shape and number of misidentified hadronic events. For the signal shape, the mean and width in $\bar{B} \to D^{(*)}\pi\ell^-\bar{\nu}_\ell$ are shifted by their respective errors obtained from the control sample, and determined to be $2-4\%$, depending on the mode. For the background shape, we estimated the uncertainty by using a different shape. For example, the main background components in $\bar{B} \to D\pi\ell^-\bar{\nu}_\ell$ are changed from $\bar{B} \to D^*\pi\ell^-\bar{\nu}_\ell$ to $\bar{B} \to D^{**}(\to D^*\pi)\ell^-\bar{\nu}_\ell$. The uncertainty is 12% for $\bar{B}^0 \to D^0\pi^+\ell^-\bar{\nu}_\ell$ due to larger background events, while it is smaller than 4% for other decay modes. For the number of misidentified hadronic events, we estimated the uncertainty to be $2-3\%$ by varying $N_{\rm bkg3}$ by its error.

The systematic error due to the uncertainty in the number of tags and amount of flavor cross-feed have to be considered as well, since the branching fraction calculation involves ratios of different B meson flavors. The former is estimated to be 4% by varying the background shapes used in the $M_{\rm bc}$ fit, and the latter is estimated to be 3% by varying the fraction of cross-feed by its error.

The effect of uncertainty on reconstruction efficiencies mostly cancels since we take the ratio to a sample that differs from the signal by only one pion. We, therefore, assign a total of 1% error due to tracking efficiency (based on a study of partially reconstructed D^* decays) and particle identification (based on a study of kinematically selected $D^{*+} \to D^0(\to K^-\pi^+)\pi^+$ decays). The uncertainty due to finite MC statistics used to model the signal is $2-3\%$.

To estimate the uncertainty in efficiency due to the modeling in the MC simulation, we compared $\bar{B} \to D^{**}(\to D^{(*)}\pi)\ell^-\bar{\nu}_\ell$ and $\bar{B} \to D^{(*)}\pi\ell^-\bar{\nu}_\ell$. The difference of 10% was assigned as the error due to this effect.

The total uncertainty is the quadratic sum of all above contributions, and amounts to $13-20\%$, depending on the mode. In the measurement of the absolute branching fractions, we quote an additional $4-10\%$ systematic error due

TABLE I. Signal yields, number of misidentified hadronic events, efficiencies, and raw branching fractions for $\bar{B} \to D^{(*)}\ell^-\bar{\nu}_\ell$, compared with their world average values. Systematic errors are not included.

Mode	$N_{\rm sig}$	$N_{\rm bkg3}$	$\epsilon(\%)$	$\mathcal{B}(10^{-2})$	PDG $\mathcal{B}(10^{-2})$
$D^0\ell^-\bar{\nu}_\ell$	1049 ± 44	9 ± 4	5.70	2.37 ± 0.10	2.15 ± 0.22
$D^{*0}\ell^-\bar{\nu}_\ell$	1419 ± 59	13 ± 4	3.02	6.06 ± 0.25	6.5 ± 0.5
$D^+\ell^-\bar{\nu}_\ell$	467 ± 26	4 ± 2	4.15	2.14 ± 0.12	2.14 ± 0.22
$D^{*+}\ell^-\bar{\nu}_\ell$	476 ± 25	3 ± 2	2.05	4.70 ± 0.24	5.44 ± 0.23

TABLE II. Signal yields, number of misidentified hadronic events, efficiencies, and statistical significance for $\bar{B} \to D^{(*)}\pi\ell^-\bar{\nu}_\ell$.

Mode	$N_{\rm sig}$	$N_{\rm bkg3}$	$\epsilon(\%)$	Σ
$D^+\pi^-\ell^-\bar{\nu}_\ell$	142.1 ± 16.5	5.7 ± 3.2	3.41	12.4
$D^{*+}\pi^-\ell^-\bar{\nu}_\ell$	62.5 ± 9.7	2.6 ± 1.8	1.38	9.9
$D^0\pi^+\ell^-\bar{\nu}_\ell$	72.0 ± 12.4	1.1 ± 1.7	4.06	8.2
$D^{*0}\pi^+\ell^-\bar{\nu}_\ell$	62.7 ± 11.6	1.7 ± 1.5	2.09	7.2

TABLE III. Ratios and branching fractions for $\bar{B} \to D^{(*)}\pi\ell^-\bar{\nu}_\ell$ decays. The first error is statistical, the second is systematic. For $\mathcal{B}$, the third error is due to the branching fraction uncertainties of $\bar{B} \to D^{(*)}\ell^-\bar{\nu}_\ell$.

Mode	R	$\mathcal{B}(10^{-2})$
$D^+\pi^-\ell^-\bar{\nu}_\ell$	$0.25 \pm 0.03 \pm 0.03$	$0.54 \pm 0.07 \pm 0.07 \pm 0.06$
$D^{*+}\pi^-\ell^-\bar{\nu}_\ell$	$0.12 \pm 0.02 \pm 0.02$	$0.67 \pm 0.11 \pm 0.09 \pm 0.03$
$D^0\pi^+\ell^-\bar{\nu}_\ell$	$0.15 \pm 0.03 \pm 0.03$	$0.33 \pm 0.06 \pm 0.06 \pm 0.03$
$D^{*0}\pi^+\ell^-\bar{\nu}_\ell$	$0.10 \pm 0.02 \pm 0.01$	$0.65 \pm 0.12 \pm 0.08 \pm 0.05$

to the error on branching fractions of the normalization modes $\bar{B} \to D^{(*)}\ell^-\bar{\nu}_\ell$.

As a cross-check an independent analysis was performed with tighter requirements on $D^{(*)}$ reconstruction, ΔE, and $M_{\rm bc}$ of the tag and a slightly different fitting procedure and efficiency calculation. Results of both analyses are consistent.

We compute the total branching fractions of $\bar{B} \to D^{(*)}\pi\ell^-\bar{\nu}_\ell$ assuming isospin symmetry, $\mathcal{B}(\bar{B} \to D^{(*)}\pi^0\ell^-\bar{\nu}_\ell) = \frac{1}{2}\mathcal{B}(\bar{B} \to D^{(*)}\pi^\pm\ell^-\bar{\nu}_\ell)$, to estimate the branching fractions of $D^{(*)}\pi^0$ final states. We obtain

$$\mathcal{B}_{D^{(*)}\pi\ell^-\bar{\nu}_\ell}(B^-) = (1.81 \pm 0.20 \pm 0.20) \times 10^{-2},$$

$$\mathcal{B}_{D^{(*)}\pi\ell^-\bar{\nu}_\ell}(\bar{B}^0) = (1.47 \pm 0.20 \pm 0.17) \times 10^{-2},$$

where the first error is statistical and the second is systematic. Our measurements are consistent with the ALEPH result and significantly smaller than that of DELPHI. This clearly shows, as suggested by ALEPH's result, that the missing branching fraction in semileptonic B decays is not fully covered by these excited states. Further searches must be carried out in $\bar{B} \to D^{(*)}\pi\pi\ell^-\bar{\nu}_\ell$ modes.

A study of the mass structure of $D^{(*)}\pi$ in $\bar{B} \to D^{(*)}\pi\ell^-\bar{\nu}_\ell$ decays is needed to understand the decay mechanics of $\bar{B} \to D^{**}\ell^-\bar{\nu}_\ell$, which would provide crucial tests of HQET and QCD sum rules [17]. Belle has recently observed all four D^{**} states (D_1', D_0^*, D_1 and D_2^*) in the hadronic B decay $\bar{B} \to D^{**}\pi$ [18]. The corresponding semileptonic decay $\bar{B} \to D^{**}\ell^-\bar{\nu}_\ell$, however, has been observed only for $\bar{B}^0 \to D_1^0(\to D^{*+}\pi^-)\ell^-\bar{\nu}_\ell$ by CLEO [19]. These contributions could be clarified by the method with fully reconstructed tags with a larger data set.

In conclusion, we have measured the branching fractions of $B^- \to D^{(*)+}\pi^-\ell^-\bar{\nu}_\ell$, and $\bar{B}^0 \to D^{(*)0}\pi^+\ell^-\bar{\nu}_\ell$. These decay modes have been clearly observed in a clean environment thanks to full reconstruction tagging, and the direct measurement of these branching fractions was achieved for the first time.

We thank the KEKB group for excellent operation of the accelerator, the KEK cryogenics group for efficient solenoid operations, and the KEK computer group and the NII for valuable computing and Super-SINET network support. We acknowledge support from MEXT and JSPS (Japan); ARC and DEST (Australia); NSFC (contract No. 10175071, China); DST (India); the BK21 program of MOEHRD, and the CHEP SRC and BR (grant No. R01-2005-000-10089-0) programs of KOSEF (Korea); KBN (contract No. 2P03B 01324, Poland); MIST (Russia); MHEST (Slovenia); SNSF (Switzerland); NSC and MOE (Taiwan); and DOE (USA).

[1] S. Eidelman *et al.*, Phys. Lett. B **592**, 1 (2004); Particle Data Group, http://pdg.lbl.gov/.
[2] D. Skulls *et al.* (ALEPH Collab.), Z. Phys. C **73**, 601 (1997).
[3] P. Abreu *et al.* (DELPHI Collab.), Phys. Lett. B **475**, 407 (2000).
[4] Examples of these measurements can be found in K. Abe *et al.* (Belle Collab.), Phys. Lett. B **526**, 247 (2004); H. Kakuno *et al.* (Belle Collab.), Phys. Rev. Lett. **92**, 101801 (2004).
[5] A. Abashian *et al.* (Belle Collab.), Nucl. Instr. and Methods Phys. Res., Sect. A **479**, 117 (2002).
[6] S. Kurokawa and E. Kikutani, Nucl. Instr. and Methods Phys. Res., Sect. A **499**, 1 (2003), and other papers included in this volume.
[7] K. Abe *et al.* (Belle Collab.), Phys. Rev. D **66**, 032007 (2002).
[8] R. Brun *et al.*, GEANT 3.21, CERN Report DD/EE/84-1 (1984).
[9] See the EvtGen package home page, http://www.slac.stanford.edu/~lange/EvtGen/.
[10] J. Duboscq *et al.* (CLEO Collab.), Phys. Rev. Lett. **76**, 3898 (1996).
[11] L. Goity and W. Roberts, Phys. Rev. D **51**, 3459 (1995).
[12] D. Scora and N. Isgur, Phys. Rev. D **52**, 2783 (1995); See also N. Isgur *et al.*, Phys. Rev. D **39**, 799 (1989).
[13] C. Fox and S. Wolfram, Phys. Rev. Lett. **41**, 1581 (1978).
[14] J. E. Gaiser *et al.*, Phys. Rev. D **34**, 711 (1986).
[15] H. Alberecht *et al.* (ARGUS Collab.), Z. Phys. C **48**, 543 (1990).
[16] H. Alberecht *et al.* (ARGUS Collab.), Z. Phys. C **57**, 533 (1993).
[17] A. Le Yaounanc *et al.*, Phys. Lett. B **520**, 25 (2001).
[18] K. Abe *et al.*, Phys. Rev. D **69**, 112002 (2004).
[19] A. Anastassov *et al.* (CLEO Collab.), Phys. Rev. Lett. **80**, 4127 (1998).